

available at www.sciencedirect.comjournal homepage: www.ejconline.com

VEGF-SPECT with ¹¹¹In-bevacizumab in stage III/IV melanoma patients

Wouter B. Nagengast ^a, Marjolijn N. Lub-de Hooge ^{c,e}, Esther M.E. van Straten ^a, Schelto Kruijff ^b, Adrienne H. Brouwers ^c, Wilfred F.A. den Dunnen ^d, Johan R. de Jong ^c, Harry Hollema ^d, Rudi A. Dierckx ^c, Nanno H. Mulder ^a, Elisabeth G.E. de Vries ^a, Harald J. Hoekstra ^b, Geke A.P. Hospers ^{a,*}

^a Department of Medical Oncology, University Medical Center Groningen, Hanzeplein 1, Postbus 30.001, 9700 RB Groningen, Netherlands

^b Department of Surgery, University Medical Center Groningen, Hanzeplein 1, Postbus 30.001, 9700 RB Groningen, Netherlands

^c Department of Nuclear Medicine and Molecular Imaging, University Medical Center Groningen, Hanzeplein 1, Postbus 30.001, 9700 RB Groningen, Netherlands

^d Department of Pathology, University Medical Center Groningen, Hanzeplein 1, Postbus 30.001, 9700 RB Groningen, Netherlands

^e Department of Hospital Pharmacy, University Medical Center Groningen, Hanzeplein 1, Postbus 30.001, 9700 RB Groningen, Netherlands

ARTICLE INFO

Article history:

Received 18 January 2011

Accepted 14 February 2011

Available online 21 March 2011

Keywords:

VEGF

Melanoma

Bevacizumab

Imaging

SPECT

Biomarker

ABSTRACT

Purpose: A feasibility study was performed to investigate the presence of VEGF in melanoma lesions by VEGF-SPECT with ¹¹¹In-bevacizumab. In addition the effect of a single therapeutic bevacizumab dose on ¹¹¹In-bevacizumab uptake was compared with VEGF levels in resected melanoma lesions.

Patients and methods: Eligible were patients with stage III/IV melanoma who presented with nodal recurrent disease. VEGF-SPECT was performed after administration of 100 Mbq ¹¹¹In-bevacizumab (8 mg) at days 0, 2, 4 and 7 post injection. Tumour visualisation and quantification were compared with CT and FDG-PET. On day 7 a single dose of 7.5 mg/kg bevacizumab was administered intravenously. On day 21, a second tracer dose ¹¹¹In-bevacizumab was administered and scans were obtained on days 21, 25 and 28. Metastases were surgically resected within 2 weeks after the last VEGF-SPECT scan and immunohistological (IHC) VEGF tumour expression was compared with ¹¹¹In-bevacizumab tumour uptake.

Results: Nine patients were included. FDG-PET and CT detected both in total 12 nodal lesions which were all visualised by VEGF-SPECT. At baseline, ¹¹¹In-bevacizumab tumour uptake varied 3-fold between and 1.6 ± 0.1-fold within patients. After a therapeutic dose of bevacizumab there was a 21 ± 4% reduction in ¹¹¹In-bevacizumab uptake. The ¹¹¹In-bevacizumab tumour uptake in the second series positively correlated with the VEGF-A expression in the resected tumour lesions.

Conclusion: VEGF-SPECT could visualise all known melanoma lesions. A single dose of bevacizumab slightly lowered ¹¹¹In-bevacizumab uptake. Future studies should elucidate the role of VEGF-SPECT in the selection of patients and the individual dosing of bevacizumab treatment.

© 2011 Elsevier Ltd. All rights reserved.

* Corresponding author: Tel.: +31 50 3616161; fax: +31 50 3614862.

E-mail address: g.a.p.hospers@int.umcg.nl (G.A.P. Hospers).

0959-8049/\$ - see front matter © 2011 Elsevier Ltd. All rights reserved.

doi:10.1016/j.ejca.2011.02.009

1. Introduction

Tumour angiogenesis, the forming of new blood vessels, is a continuous process which allows tumour cells to execute their critical growth by supplying the tumour with nutrients and oxygen, disposing of metabolic waste products and providing a route for metastatic spreading.^{1,2} Vascular endothelial growth factor A (VEGF-A) is one of the key growth factors involved in the development and maintenance of tumour angiogenesis.³ Bevacizumab, a fully humanised monoclonal antibody, binds to all VEGF-A isoforms with high affinity and thereby blocks ligand–receptor signalling.⁴ Bevacizumab is currently used in patients with tumours such as metastatic colon cancer, renal cell cancer and breast cancer.^{5–7}

Melanoma causes more than 75% of all skin cancer deaths. Melanoma features a specific metastatic spread from primary tumour to regional lymphatic beds and then distant metastases.^{8,9} When patients present with lymph node or distant metastases their prognosis is worse, with 5 year survival rates of, respectively, 47% and 10%.^{10,11}

Several factors point to a role for VEGF in melanoma. Melanoma cells produce high amounts of VEGF-A which correlates with advanced disease, tumour burden, poor overall survival and probability of progression.¹² Furthermore, VEGF-A expression in nodal metastases is higher compared to primary tumours indicating the importance of a pro-angiogenic switch in the process of melanoma progression.⁸ In addition, pre-clinical studies in mice have demonstrated up-regulation of pro-inflammatory chemokines in the lung parenchyma by VEGF-A production of the primary melanoma lesion, thereby contributing to the process defined as ‘seed and soil’ of metastasis.^{13,14} For these reasons, the use of anti-VEGF targeted therapies is of potential interest in the treatment of melanoma patients. The first clinical studies in metastatic melanoma patients showed low activity of VEGF-A antibody bevacizumab combined with interferon-2 α , but encouraging responses have been observed clinically when bevacizumab was combined with chemotherapy.^{15–18}

Currently, no biomarkers are available to determine the presence of a drug target for anti-angiogenic drugs across tumour lesions in patients to predict anti-tumour efficiency. A potentially attractive method is the use of non-invasive visualisation of *in vivo* biological processes by nuclear medicine imaging techniques. A new option in this field is molecular VEGF imaging. VEGF consists of at least four splice variants, containing 121, 165, 189 and 206 amino acids.³ VEGF₁₂₁ is freely soluble, VEGF₁₆₅ is partly secreted, while a significant fraction remains localised to the extra cellular matrix and cell surface, like VEGF₁₈₉ and VEGF₂₀₆ resulting in high concentrations in the tumour micro-environment.^{19–23} These isoforms are attractive imaging targets for VEGF imaging as this could provide non-invasively insight in the local VEGF status and thereby be useful to guide anti-angiogenic therapy. Recently, tumour visualisation and *in vivo* measurement of VEGF tumour levels was made possible by using radionuclide VEGF imaging.^{24–28} Pre-clinically we demonstrated that the uptake of radiolabelled bevacizumab correlated with *ex vivo* VEGF

levels of the tumour as determined by ELISA in tumour lysates at baseline and after treatment with a Heat Shock Protein 90 (HSP90) inhibitor.²⁹

In the present study we investigated the feasibility of VEGF visualisation and quantification of melanoma lesions as molecular target with SPECT using ¹¹¹In-bevacizumab as tracer.³⁰ In addition the effect of a single therapeutic bevacizumab dose on ¹¹¹In-bevacizumab uptake was compared with VEGF levels in the resected melanoma lesions.

2. Patients and methods

2.1. Patients

All eligible patients who visited the outpatient clinics of the University Medical Centre Groningen (UMCG) between November-2007 till June-2009 were offered participation in the trial. Eligible patients were ≥ 18 years of age, had a WHO performance status of 0–2, with stage III/IV melanoma who presented with nodal recurrent disease. They were excluded in case of prior immuno- or chemotherapy for metastatic disease, prior radiotherapy on the involved area or major surgery within 28 days of start of the study, any investigational drug within 30 days before start of the study, or clinical evidence of brain metastases.

Routine staging included a complete history, physical examination, and blood chemistry profile, in addition to CT-scan and FDG-PET scan. The study was approved by the local medical ethics committee and written informed consent was obtained from all participants. The study was registered under trial number NTR1941.

2.2. Study design

In the first 3 patients after ¹¹¹In-bevacizumab administration VEGF-SPECT scanning was evaluated at days 0, 2, 4 and 7. Hereafter patients were scanned at days 0, 4 and 7 post injection. On day 7 the patients received a single dose of 7.5 mg/kg bevacizumab intravenously. On day 21, a second tracer dose ¹¹¹In-bevacizumab was administered and scans were obtained on days 21, 25 and 28. Patients were operated within 2 weeks after the last ¹¹¹In-bevacizumab scan.

2.3. VEGF-SPECT

Bevacizumab was conjugated with the chelator 2-(4-isothiocyanatobenzyl)-diethylenetriaminepentaacetic acid (ITC-DTPA) (Macrocyclics) as described previously.²⁴ One batch of ITC-DTPA-bevacizumab conjugate was produced. This batch was tested for conjugation ratio, efficiency of the labelling, pH, immunoreactive fraction (VEGF binding ELISA), sterility and apyrogenicity as described previously.²⁴ The purified conjugated bevacizumab was diluted (10 mg/mL) in ammonium acetate and stored at -80°C . ¹¹¹In labelling was performed separately for each patient. The final product had a radiochemical purity of $\geq 95\%$, was sterile and free from pyrogens. The conjugation and labelling procedures were validated and performed under good manufacturing practice conditions.

Scintigraphy was performed after administration of 100 ± 3 Mbq ^{111}In -bevacizumab (8 mg bevacizumab). Planar whole body imaging was performed, using a two-headed gamma camera, equipped with parallel-hole medium-energy collimators, at a scan speed of 10 cm/min (days 0 and 2 post injection (pi)) or 5 cm/min (days 4 and 7 pi) and stored digitally in a 256×1024 matrix. SPECT images were obtained from pre-defined tumour lesions, using 180° sampling with 32 projections per head, 45 s acquisition time per projection and a 128×128 matrix size.

2.4. Image and data analysis

SPECT reconstructions were performed with the ordered subset expectation maximisation algorithm (OSEM). VEGF-SPECT images were fused manually with conventional CT images to validate regions of increased ^{111}In -bevacizumab uptake. Tumour uptake quantification was performed with AMIDE Medical Image Data Examiner software (version 0.9.1, Stanford University).³¹ Quantification was performed using the day 4 scan which showed optimal tumour to background ratios. For the quantification of radioactivity within the tumour, 3D volumes of interest (VOIs) were drawn within the fused VEGF-SPECT/CT image. ^{111}In -bevacizumab tumour accumulation was semi-quantitative analysed as counts per voxel as quantified by AMIDE software. Both maximum uptake and mean tumour uptake were assessed. The mean reflects the mean value over all voxels, and the max reflects the maximum voxel value in the tumour. Since all patients received 100 Mbq of ^{111}In -bevacizumab and all patients were scanned at matching times on day 4 no corrections performed for attenuation and injected dose for quantification of SPECT images. ^{18}F -FDG quantification was performed as described previously using the AMIDE; the Standardised Uptake Value (SUV) was calculated according to the following formula: $\text{SUV} = \text{radioactivity concentration in the tissue (Bq/kg)} / (\text{injected dose (Bq)} / \text{patient weight (kg)})$ (30). Three dimensional VOIs were placed semi-automatically by using a threshold of 40% of the maximum value (SUV_{max}) in a pre-selected region.

2.5. Immunohistochemistry

Both resected melanoma lesions and primary melanoma samples obtained at initial diagnosis (range 2 months to 7 year), were analysed. Single and double immunofluorescence staining was performed on $3 \mu\text{m}$ -thick paraffin-embedded tumour slides with selected combinations of the primary antibodies rabbit anti-VEGF-A (A20-sc152, 1:50, Santa Cruz) which binds the N-terminus of VEGF-A of human origin, mouse anti-Ki67 (1:300, clone MIB-1, Dako) and mouse anti-Hif1 α (1:100, clone 54, BD Biosciences). Immunosignals were visualised using combinations of goat anti-mouse AlexaFluor 660 antibodies, donkey anti-rabbit AlexaFluor 488 antibodies or goat anti-mouse AlexaFluor 488 antibodies (1:400, all from Invitrogen). Nuclear staining was performed with bisbenzimidazole H 33258 fluorochrome (1:5000, Merck, Darmstadt, Germany). Slides were analysed using a Leica DMRXA immunofluorescence microscope equipped with appropriate excitation and emission filters for maximum separation of Alexa Fluor 488 (e.g.

FITC), Alexa Fluor 660 (e.g. TRITC), and H33258 (e.g. DAPI). Images were captured with a Leica DC350 FX camera. Leica QWinPro software was used for evaluation of the slides (all from Leica Microsystems). VEGF-A and HIF1 α intensity (value 1–5), was scored at $400\times$ magnification in 3 tumour areas defined as hot spot areas. The proliferation index was calculated by percentage of Ki67 positive cells in at least 3 high power fields ($400\times$).

2.6. Statistical analysis

Data are presented as means \pm standard error of the mean (SEM). Statistical analysis was performed using the Mann–Whitney test for non-parametric data or a paired sampled T-test for paired data (SPSS, version 14). Associations between parameters were evaluated using Pearson's correlation test. A double side P-value ≤ 0.05 was considered significant.

3. Results

3.1. Patients characteristics

Nine patients were included, average age 51.5 years (29–62 years). The primary melanoma was diagnosed between 3 months and 7 years ago before inclusion in the study. In these patients, 12 lymph node lesions were detected with CT as well as with FDG-PET imaging. No discrepancy existed between these imaging modalities. Six patients had 1 melanoma lesion, three patients had 2 lesions. In patients with more than 1 lesion, melanoma lesions were located in the same region of the body. No distant metastases, like liver or bone metastases, were detected. A 4.6-fold difference existed between SUV FDG-PET uptake among lesions, suggesting large differences in metabolic activity.

3.2. VEGF-SPECT tumour visualisation at baseline

Directly after the first tracer administration, ^{111}In -bevacizumab was mainly located in the circulation and well perfused organs like heart and liver. As shown in Fig. 1A, ^{111}In -bevacizumab activity in the circulation decreased from day 0 to day 7, whereas ^{111}In -bevacizumab tumour uptake increased. Tumour lesions became clearly visible from day 2 onwards, with increasing tumour to background ratios over time. At day 7, decay of ^{111}In resulted in relatively low count rates and therefore inferior image quality compared to day 4. For this reason, we concluded that day 4 after ^{111}In -bevacizumab injection was optimal for visualisation and quantification of ^{111}In -bevacizumab uptake in the tumour. No infusion related reactions or adverse events were noticed during the study.

VEGF-SPECT imaging detected all known CT and FDG-PET lesions. Even small tumour, smaller than 16 mm in diameter, lesions were visualised by VEGF-SPECT (Fig. 2A). No new lesions were detected by VEGF-SPECT.

3.3. Quantification of VEGF-SPECT at baseline

Semi-quantitative analyses of the SPECT images demonstrated a linear relation between maximum and mean

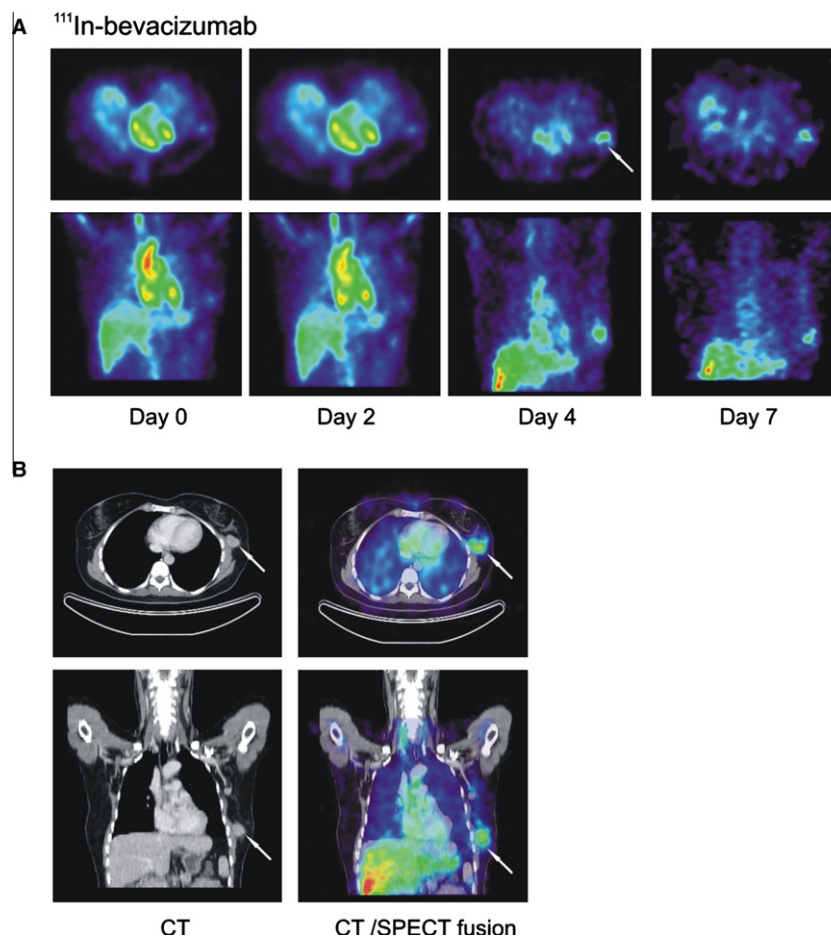


Fig. 1 – (A) Transversal and coronal VEGF-SPECT images at days 0, 2, 4 and 7 post injection of the tracer. Over time, ¹¹¹In-bevacizumab accumulates in the tumour with optimal tumour to background ratio 4 days post injection. (B) Transversal and coronal CT images and VEGF-SPECT/CT fusion 4 days post injection.

¹¹¹In-bevacizumab uptake was observed (respectively, $r^2 = 0.96$, $P < 0.0001$), which suggest a small variability caused by the used method. For this reason further analysis was performed using maximum tumour uptake value, which is not influenced by individual drawing of VOIs.

When we quantified the ¹¹¹In-bevacizumab tumour uptake, 3-fold differences in ¹¹¹In-bevacizumab maximum tumour uptake were observed between patients, suggesting large differences in VEGF levels (Fig. 3A). Moreover, in individual patients, 1.6 ± 0.1 -fold differences in maximum ¹¹¹In-bevacizumab tumour uptake existed between tumour lesions. In one patient VEGF-SPECT demonstrated inhomogeneous tumour uptake within a melanoma lesion, 5.4×3.2 cm in size on CT (Fig. 2C). No correlation existed between the ¹¹¹In-bevacizumab uptake and the ¹⁸F-FDG tumour uptake ($r^2 = 0.38$, $P = 0.10$).

3.4. VEGF-SPECT following therapeutic administration of bevacizumab

All known melanoma lesions were still detectable with VEGF-SPECT 2 weeks after therapeutic administration of bevacizumab. With the exception of one lesion, all other lesions (11 out of 12) showed a reduction in ¹¹¹In-bevacizumab

tumour uptake, resulting in an average decline of $21 \pm 4\%$ ($P = 0.002$) compared to the baseline scan (Fig. 3B). Differences existed in the relative and absolute change in ¹¹¹In-bevacizumab uptake between lesions, ranging from +2% to -42%, and +1 to -29 counts per voxel compared to the first scan series (Fig. 3A and B). No correlation was found between the baseline uptake and the relative (%) change in ¹¹¹In-bevacizumab tumour uptake ($r^2 = 0.22$, $P = 0.11$).

3.5. Immunohistochemistry

All primary melanomas and lymph node metastasis had a positive VEGF-A staining, though staining intensities ranged from weak to strong between patients (Fig. 4A and B). Five patients had a weak staining (score 1–2), two patients a moderate staining (score 3) and two patients a strong staining (score 4–5). The VEGF-A staining in the resected melanoma lesions correlated with the ¹¹¹In-bevacizumab tumour uptake after a bevacizumab therapeutic dose, performed within 2 weeks before surgical resection (Pearson $r = 0.75$, $P = 0.017$) (Fig. 4C). In contrast, no correlation was found between the VEGF-A staining in the primary melanoma samples and baseline ¹¹¹In-bevacizumab uptake ($P = 0.38$). In addition, no correlation was found between ¹¹¹In-bevacizumab tumour uptake

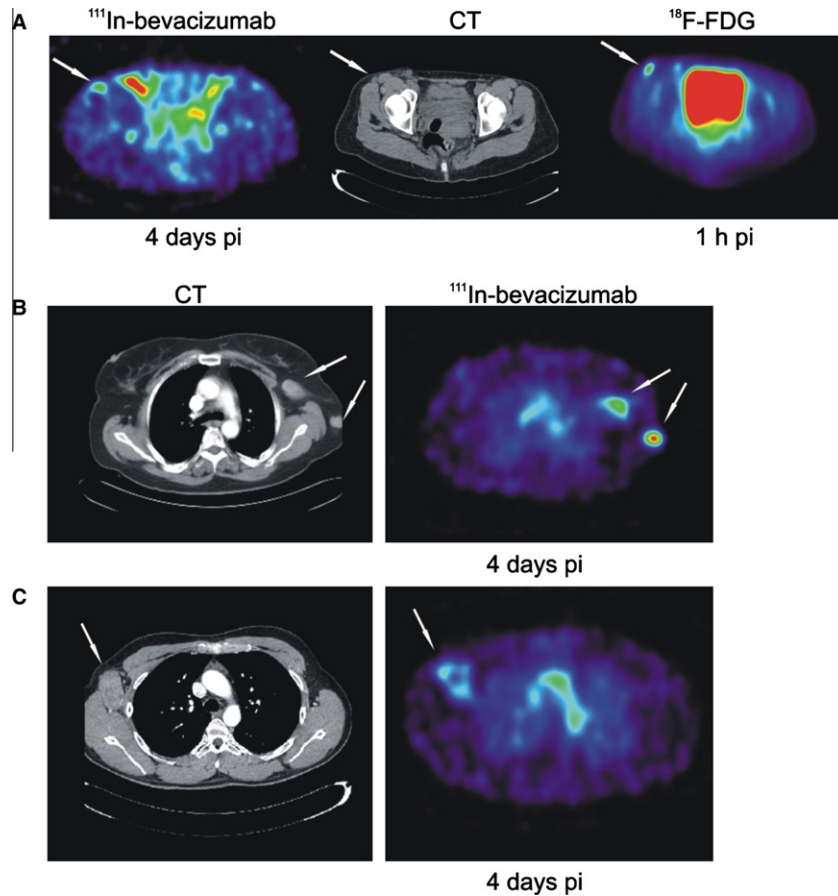


Fig. 2 – (A) Small melanoma lesions, 16 mm in diameter on CT, detection by ¹¹¹In-bevacizumab, CT imaging and FDG imaging. (B) Differential ¹¹¹In-bevacizumab uptake between two melanoma lesions. (C) Inhomogeneous ¹¹¹In-bevacizumab tumour uptake in melanoma lesion.

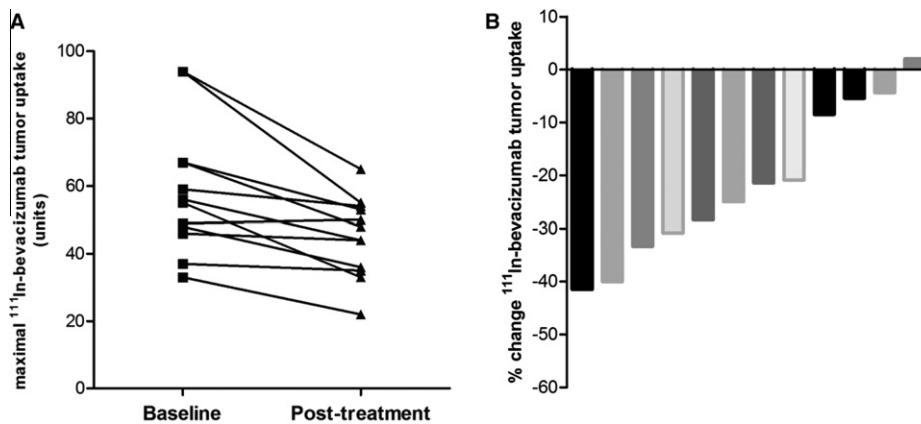


Fig. 3 – (A) Maximal ¹¹¹In-bevacizumab tumour uptake pre- and post-administration of 7.5 mg/kg bevacizumab. (B) Waterfall plot of percentage change in ¹¹¹In-bevacizumab uptake following 7.5 mg/kg bevacizumab administration of different lesions.

and HIF1 α staining ($P = 0.11$) and Ki67 tumour proliferation ($P = 0.72$) in the resected lymph node metastases.

4. Discussion

In the present study we demonstrated that VEGF-SPECT visualised all known melanoma lymph node lesions identified by

CT and FDG-PET imaging. At baseline there was a large variation in ¹¹¹In-bevacizumab tumour uptake between patients, across lesions within a patient and within lesions. This suggests differential presence of drug target for anti-VEGF targeted drugs between melanoma patients and between lesions within a patient which was confirmed by immunohistochemistry. A subsequent single dose of 7.5 mg/kg

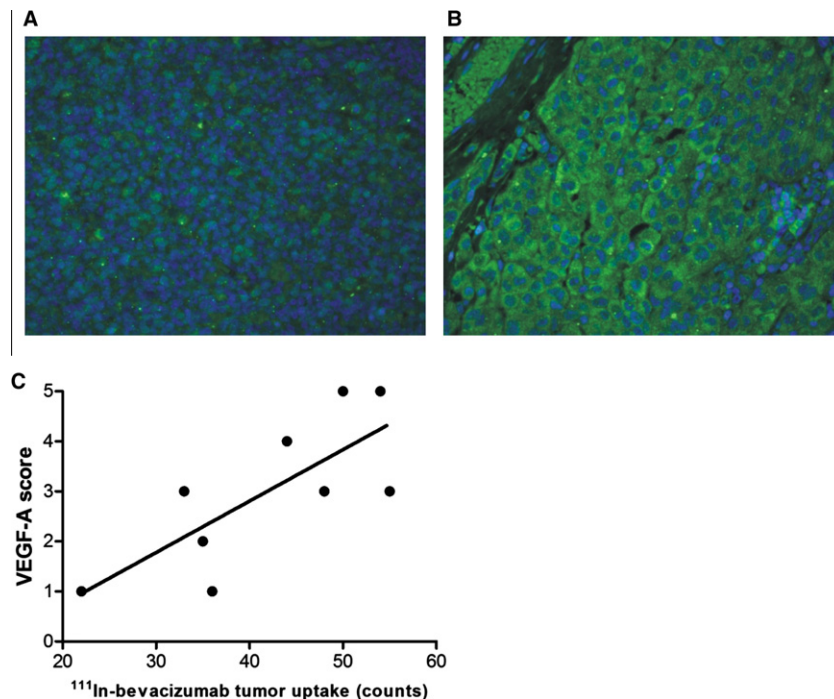


Fig. 4 – Weak (A) and strong (B) VEGF-A immunofluorescent staining of melanoma lesions two weeks after 7.5 mg/kg bevacizumab treatment. (C) Correlation between ^{111}In -bevacizumab tumour uptake of second scan series and VEGF-A immunofluorescent staining in resected melanoma lesions.

bevacizumab resulted in a slight decrease of ^{111}In -bevacizumab uptake in the second scan series. Moreover, ^{111}In -bevacizumab uptake in the second scan series prior to surgical resection, nicely correlated with the VEGF-A expression assessed by immunohistochemistry of the resected melanoma lesions, thus giving non-invasively insight in the local VEGF status.

To date, two anti-VEGF antibodies have been used for the clinical VEGF imaging: HumMV833 and bevacizumab.^{24,25,32,33} Jayson et al. used ^{124}I -HuMV833, a humanised monoclonal IgG₄ antibody that binds VEGF₁₂₁ and VEGF₁₆₅, to perform PET-imaging studies in patients with various progressive solid tumours.³² Tumour uptake of ^{124}I -HuMV833 was highly variable between and within patients. For example, there was high uptake of ^{124}I -HuMV833 in an ovarian tumour and low uptake in a poorly vascularised metastasis in a colon cancer patient.³² These differences likely reflect the variation in VEGF secretion among tumour types and lesions. ^{111}In - and ^{89}Zr -bevacizumab showed specific tumour uptake in human ovarian, colon and melanoma xenograft models.^{24,25,27} In contrast to our findings, Scheer et al. did not find a correlation between the uptake of ^{111}In -bevacizumab and VEGF levels in liver metastases.²⁸ This could likely be explained by the fact that semi-quantitative 2D planar scintigraphy was used as comparison with the *ex vivo* ELISA data. This results in a lower sensitivity for the detection of tumour lesions and does not allow 3D quantification as with SPECT data. In addition, quantification of liver metastases was presumably hampered by the large endogenous liver uptake of ^{111}In -bevacizumab resulting in relative low tumour to background ratios.

In the present study we observed optimal tumour to background ratios 4 days post injection of ^{111}In -bevacizumab in melanoma patients, which is in concordance with ^{111}In radiolabelled trastuzumab, reflecting the relatively slow pharmacokinetics of monoclonal antibodies.³⁴ Directly after injection, ^{111}In -bevacizumab is mainly present in the circulation and well perfused organs. Non-specific liver uptake was seen for ^{111}In -bevacizumab, and was comparable to other radiolabelled antibodies, for example ^{111}In -trastuzumab.³⁴ Due to the relatively slow clearance of ^{111}In -bevacizumab, extended tumour exposure takes place which results in maximal tumour accumulation whereas non-specific uptake in other organs decreases over time. In addition, the high production of VEGF by the tumour and subsequent high VEGF concentration in the micro-environment presumably lead to sensitive detection of tumour lesions by VEGF-SPECT. For these reasons, even lesions of around 1.5 cm in diameter were detectable. Here the high sensitivity might be facilitated by the low antibody uptake of the surrounding tissue of the lymph node metastasis. Most likely, radiolabelled bevacizumab binds to all VEGF-A isoforms located on the cell surface and the extracellular matrix as has been proven pre-clinically in VEGF₁₆₅ and VEGF₁₈₉ over-expressing melanoma xenografts.²⁷

When we looked at individual tumour lesions at baseline, large differences were detected in ^{111}In -bevacizumab uptake. This could be of interest since it has been shown that VEGF and VEGF-receptor (VEGFR) expression in melanomas are associated with disease progression and response to anti-angiogenic treatment.^{35,36} For instance, in melanoma patients response to sorafenib, a pan-VEGFR tyrosine kinase inhibitor, was associated with high VEGFR2 expression in the tumour

before treatment as measured by immunohistochemistry.³⁵ Unfortunately, few tumour lesions are accessible for biopsy. Therefore, there is a need for a non-invasive method to assess the angiogenic state of the tumour. VEGF imaging could facilitate in this.

In our study VEGF-SPECT quantification, obtained within 2 weeks prior to surgery, correlated with *ex vivo* VEGF-A staining of the resected melanoma lesions. These findings suggest VEGF driven uptake and the possibility to non-invasively monitor VEGF levels in the tumour micro-environment. We did not find a correlation between baseline ¹¹¹In-bevacizumab uptake and VEGF staining in the primary melanoma. This could well be due to the time between the biopsy of the primary tumour and disease progression. For instance, it has been shown that VEGF-A expression in nodal metastases is higher compared to primary tumours.⁸ For this reason, assessment of VEGF levels in primary melanoma lesions likely is not informative for the VEGF status in the metastases.

VEGF-SPECT imaging post-administration of a therapeutic bevacizumab dose resulted in an average decrease of 21% in ¹¹¹In-bevacizumab tumour uptake. This decrease could be due to blockade of the target by therapeutic bevacizumab and thereby hamper ¹¹¹In-bevacizumab binding to matrix bound VEGF. Pre-clinically, increasing doses of unlabelled bevacizumab could lower the uptake of ¹¹¹In-bevacizumab in a human xenograft model.²⁵ At the time of the second ¹¹¹In-bevacizumab administration, around 60–70% of the cold bevacizumab is still present in the circulation. Secondly, in animal and clinical studies bevacizumab treatment rapidly induced vascular changes like decreased vascular density and permeability.^{37,38} This phenomenon could lead to lower ¹¹¹In-bevacizumab tumour penetration. For these reasons, VEGF imaging could give functional information after anti-angiogenic treatment and be a biomarker, especially combined with CT-imaging when also anatomic information is obtained like with SPECT-CT or PET-CT imaging. Use of the currently available PET tracer ⁸⁹Zr-bevacizumab, allowing high resolution whole body quantitative PET imaging compared to semi-quantitative SPECT imaging, might well further potentiate this imaging approach.²⁴

In conclusion, VEGF-SPECT is a feasible clinical imaging modality for the visualisation of melanoma lymph node metastases. VEGF-SPECT visualisation and quantification is a potential non-invasive biomarker in the selection of tumours that have high expression levels of VEGF and the individual dosing of bevacizumab treatment.

Conflict of interest statement

None declared.

REFERENCES

1. Folkman J. What is the evidence that tumors are angiogenesis dependent? *J Natl Cancer Inst* 1990;**82**:4–6.
2. Folkman J, Klagsbrun M. Angiogenic factors. *Science* 1987;**235**:442–7.
3. Ferrara N, Davis-Smyth T. The biology of vascular endothelial growth factor. *Endocr Rev* 1997;**18**:4–25.
4. Gerber HP, Ferrara N. Pharmacology and pharmacodynamics of bevacizumab as monotherapy or in combination with cytotoxic therapy in preclinical studies. *Cancer Res* 2005;**65**:671–80.
5. Gaudreault J, Fei D, Rusit J, Suboc P, Shiu V. Preclinical pharmacokinetics of ranibizumab (rhuFabV2) after a single intravitreal administration. *Invest Ophthalmol Vis Sci* 2005;**46**:726–33.
6. Miller K, Wang M, Gralow J, et al. Paclitaxel plus bevacizumab versus paclitaxel alone for metastatic breast cancer. *N Engl J Med* 2007;**357**:2666–76.
7. Sandler A, Gray R, Perry MC, et al. Paclitaxel-carboplatin alone or with bevacizumab for non-small-cell lung cancer. *N Engl J Med* 2006;**355**:2542–50.
8. Gorski DH, Leal AD, Goydos JS. Differential expression of vascular endothelial growth factor-A isoforms at different stages of melanoma progression. *J Am Coll Surg* 2003;**197**:408–18.
9. Tas F, Duranyildiz D, Oguz H, et al. Circulating serum levels of angiogenic factors and vascular endothelial growth factor receptors 1 and 2 in melanoma patients. *Melanoma Res* 2006;**16**:405–11.
10. Bastiaannet E, Oyen WJ, Meijer S, et al. Impact of [¹⁸F]fluorodeoxyglucose positron emission tomography on surgical management of melanoma patients. *Br J Surg* 2006;**93**:243–9.
11. Sekulic A, Haluska Jr P, Miller AJ, et al. Malignant melanoma in the 21st century: the emerging molecular landscape. *Mayo Clin Proc* 2008;**83**:825–46.
12. Ugurel S, Rappel G, Tilgen W, Reinhold U. Increased serum concentration of angiogenic factors in malignant melanoma patients correlates with tumor progression and survival. *J Clin Oncol* 2001;**19**:577–83.
13. Psaila B, Lyden D. The metastatic niche: adapting the foreign soil. *Nat Rev Cancer* 2009;**9**:285–93.
14. Hiratsuka S, Watanabe A, Aburatani H, Maru Y. Tumour-mediated upregulation of chemoattractants and recruitment of myeloid cells predetermines lung metastasis. *Nat Cell Biol* 2006;**8**:1369–75.
15. Varker KA, Biber JE, Kefauver C, et al. A randomised phase 2 trial of bevacizumab with or without daily low-dose interferon alfa-2b in metastatic malignant melanoma. *Ann Surg Oncol* 2007;**14**:2367–76.
16. Gonzalez-Cao M, Viteri S, Diaz-Lagares A, et al. Preliminary results of the combination of bevacizumab and weekly paclitaxel in advanced melanoma. *Oncology* 2008;**74**:12–6.
17. Terheyden P, Hofmann MA, Weininger M, Brocker EB, Becker JC. Anti-vascular endothelial growth factor antibody bevacizumab in conjunction with chemotherapy in metastasising melanoma. *J Cancer Res Clin Oncol* 2007;**133**:897–901.
18. Perez DG, Suman VJ, Fitch TR, et al. Phase 2 trial of carboplatin, weekly paclitaxel, and biweekly bevacizumab in patients with unresectable stage IV melanoma: a North Central Cancer Treatment Group study, N047A. *Cancer* 2009;**115**:119–27.
19. Ferrara N. Vascular endothelial growth factor: basic science and clinical progress. *Endocr Rev* 2004;**25**:581–611.
20. Shibuya M. Vascular endothelial growth factor receptor-2: its unique signaling and specific ligand, VEGF-E. *Cancer Sci* 2003;**94**:751–6.
21. Crawford SE. Vascular interference: a blockade to tumor epithelial growth. *Hepatology* 2004;**39**:1491–4.
22. Ferrara N. Role of vascular endothelial growth factor in regulation of physiological angiogenesis. *Am J Physiol Cell Physiol* 2001;**280**:C1358–66.

23. Park JE, Keller GA, Ferrara N. The vascular endothelial growth factor (VEGF) isoforms: differential deposition into the subepithelial extracellular matrix and bioactivity of extracellular matrix-bound VEGF. *Mol Biol Cell* 1993;4:1317–26.
24. Nagengast WB, De Vries EG, Hospers GA, et al. *In vivo* VEGF imaging with radiolabelled bevacizumab in a human ovarian tumor xenograft. *J Nucl Med* 2007;48:1313–9.
25. Stollman TH, Scheer MG, Leenders WP, et al. Specific imaging of VEGF-A expression with radiolabelled anti-VEGF monoclonal antibody. *Int J Cancer* 2008;122:2310–4.
26. Chang SK, Rizvi I, Solban N, Hasan T. *In vivo* optical molecular imaging of vascular endothelial growth factor for monitoring cancer treatment. *Clin Cancer Res* 2008;14:4146–53.
27. Stollman TH, Scheer MG, Franssen GM, et al. Tumor accumulation of radiolabelled bevacizumab due to targeting of cell- and matrix-associated VEGF-A isoforms. *Cancer Biother Radiopharm* 2009;24:195–200.
28. Scheer MG, Stollman TH, Boerman OC, et al. Imaging liver metastases of colorectal cancer patients with radiolabelled bevacizumab: lack of correlation with VEGF-A expression. *Eur J Cancer* 2008;44:1835–40.
29. Nagengast WB, de Korte MA, Oude Munnink TH, et al. ⁸⁹Zr-bevacizumab PET of early antiangiogenic tumor response to treatment with HSP90 inhibitor NVP-AUY922. *J Nucl Med* 2010;51:761–7.
30. http://www.nccn.org/professionals/physician_gls/f_guidelines.asp.
31. Loening AM, Gambhir SS. AMIDE: a free software tool for multimodality medical image analysis. *Mol Imaging* 2003;2:131–7.
32. Jayson GC, Zweit J, Jackson A, et al. Molecular imaging and biological evaluation of HuMV833 anti-VEGF antibody: implications for trial design of antiangiogenic antibodies. *J Natl Cancer Inst* 2002;94:1484–93.
33. Collingridge DR, Carroll VA, Glaser M, et al. The development of [(124)I]iodinated-VG76e: a novel tracer for imaging vascular endothelial growth factor *in vivo* using positron emission tomography. *Cancer Res* 2002;62:5912–9.
34. Perik PJ, Lub-De Hooge MN, Gietema JA, et al. Indium-111-labeled trastuzumab scintigraphy in patients with human epidermal growth factor receptor 2-positive metastatic breast cancer. *J Clin Oncol* 2006;24:2276–82.
35. Jilaveanu L, Zito C, Lee SJ, et al. Expression of sorafenib targets in melanoma patients treated with carboplatin, paclitaxel and sorafenib. *Clin Cancer Res* 2009;15:1076–85.
36. Straume O, Akslen LA. Expression of vascular endothelial growth factor, its receptors (FLT-1, KDR) and TSP-1 related to microvessel density and patient outcome in vertical growth phase melanomas. *Am J Pathol* 2001;159:223–35.
37. O'Connor JP, Carano RA, Clamp AR, et al. Quantifying antivascular effects of monoclonal antibodies to vascular endothelial growth factor: insights from imaging. *Clin Cancer Res* 2009;15:6674–82.
38. Willett CG, Boucher Y, di Tomaso E, et al. Direct evidence that the VEGF-specific antibody bevacizumab has antivascular effects in human rectal cancer. *Nat Med* 2004;10:145–7.